Strain responsive concave and convex microlens arrays

Dinesh Chandra and Shu Yang[a)]
Department of Materials Science and Engineering, University of Pennsylvania, 3231 Walnut Street, Philadelphia, Pennsylvania 19104, USA

Pei-Chun Lin
Department of Mechanical Engineering, National Taiwan University No. 1, Sec. 4, Roosevelt Road, Taipei 10617, Taiwan

(Received 15 August 2007; accepted 1 December 2007; published online 20 December 2007)

We report the fabrication of single-component, strain responsive microlens arrays with real-time tunability. The concave lens array is fabricated by patterning hard oxide layer on a bidirectionally prestretched soft elastomer, poly(dimethylsiloxane) (PDMS) followed by confined buckling upon release of the prestrain. The convex microlens array is replica molded from the concave lenses in PDMS. Due to difference in lens formation mechanisms, the two types of lenses show different tunable range of focal length in response to the applied strain: large focal length change is observed from the concave microlens array, whereas that from the convex microlens array is much smaller. © *2007 American Institute of Physics*. [DOI: 10.1063/1.2827185]

With advances in miniaturization, microlens arrays play an important role in optical communication, biomedical imaging, photolithography, and biochemical sensing.[1,2] Variable-focus microlens arrays are of particular interest for microelectromechanical systems (MEMS) and sensors. A wide variety of tuning mechanisms have been reported, including responsive hydrogels,[3] electrowetting,[4] liquid pressure to deform an elastomeric membrane,[5] liquid crystal microlens arrays,[6] and integrated microfluidic channels,[7] to tune lens shape, refractive index, and the surrounding medium. Nevertheless, most of these microlens arrays are multicomponent systems, and require complex fabrication and assembly processes. Often times, the lens focal length cannot be tuned continuously in real time.

In this paper, we report the fabrication of a single-component, strain responsive, microlens array (both concave and convex) with real-time tunable focus. The concave lens array is created by confined buckling of a soft elastomer, poly(dimethylsiloxane) (PDMS), which is mechanically stretched in plane bidirectionally[8] and patterned with a thin layer of hard oxide on top. Due to extreme moduli mismatch between the hard silicate layer and the soft PDMS ($E=2$ MPa), buckling occurs upon release of prestrained bilayer film, forming wrinkled patterns spontaneously.[8,9] If the oxidation and, thus, buckling is confined to an area smaller than the wavelength of the unconfined wrinkles, microlens structure will be obtained.[10] Previously, similar strategy has been used to create microlens array by swelling a patterned oxide/PDMS bilayer structure with acrylate monomers, followed by polymerization.[10] Such formed lenses are rigid and not tunable. Because the microlens array in our system is created by mechanical stretching induced buckling, the lens shape can be reversibly tuned in real time by simply applying mechanical strain.

Briefly, the microlens array was fabricated as the following. A flat PDMS sheet with thickness of 0.5 mm was prepared by mixing PDMS precursor (RTV 615, GE Silicone) and curing agent (10:1 wt/wt) between two glass slides separated by spacers, followed by thermal curing at 65 °C for 4 h. The PDMS strip was clamped on four edges [Fig. 1(a)], leaving a center space of 25×25 mm^2 and then stretched to 20% strain in both planar directions simultaneously [Fig. 1(b)]. One side of the stretched PDMS surface was masked with a transmission electron microscopy (TEM) copper grid [Fig. 1(c)] with hexagonally packed hole array (diameter of 37 μm and hole to hole distance of 62 μm) for ultraviolet ozone (UVO) treatment (UVO-Cleaner Model 42, Jelight Company, Inc.) for 30 min [Fig. 1(d)] to generate a thin silicate layer on the exposed regions. The area surrounding the TEM grid and the backside of PDMS film were covered by scotch tape. The mask was then removed after UVO [Fig. 1(e)] and the PDMS strip was strain released in both planar directions simultaneously, resulting in a concave microlens array [Fig. 1(f)]. In the range of prestrain levels (10%–30%) and UVO treatment time (15–60 min), concave lenses were always observed. One possible explanation could be that during the strain release process, the pure PDMS surrounding the much stiffer oxidized PDMS is pushed out due to compressive forces, which favors buckling of the oxidized PDMS inwards rather than outwards. Once the oxidized layer is slightly buckled inwards, it continues to buckle in the same direction, resulting in formation of concave microlens array. To obtain the convex microlens array, we replica molded the concave microlens array in PDMS.

The fabricated microlenses appeared very uniform [Figs. 2(a) and 2(c)]. The lens diameter D and thickness h for the concave microlens array were measured by atomic force microscope (AFM) as 45.9 and 1.53 μm, respectively, whereas the corresponding values for the convex microlens array were a bit larger, 46.3 and 2 μm, respectively. The lens diameter D is much larger than the diameter of the holes in the copper grid, 37 μm. We suspect this is because (1) the contact between the TEM grid and PDMS sheet may not be completely flat, especially around the grid edge, and (2) the ozone could diffuse through the copper grid to some extent, resulting in larger lenses.

The focal length of the microlens array at various mechanical strains was measured by optical microscope (Olym-

[a)]Electronic mail: shuyang@seas.upenn.edu.

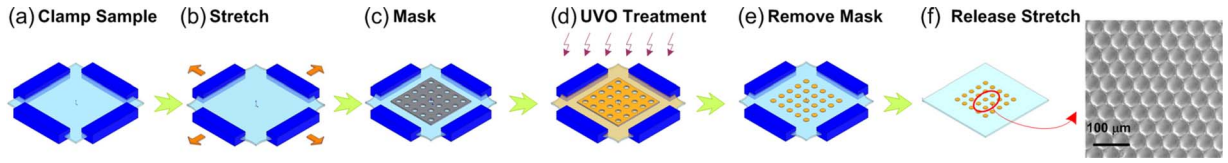

FIG. 1. (Color online) Schematic illustrations of the fabrication procedure of concave microlens array [(a)–(f)]. (f) Inset: scanning electron microscopy image of a concave microlens array.

pus BX-61) equipped with internal Z motor (resolution of 1 μm). Alphabet "N" was printed on a transparency and placed several centimeters below the microlens array [Fig. 2(e)]. First, the microlens array was brought into focus of the microscope objective [Figs. 2(b) and 2(d)], and then the image of "N" through the microlens array was brought into focus [Figs. 2(b) and 2(d), inset]. The difference between the sample-stage positions of the two foci gave the focal length of the microlens array. Since the lens profile (D and h) is uniform over the microlens array, a single focus is obtained over the entire array [Figs. 2(b) and 2(d), inset]. Here, real focus is obtained for convex lens array, but virtual focus for concave lens array.

While the nonconfined ripples have sinusoidal profile, here, for the simplicity of estimation of the lens focal length, we assume the lenses are spherical with a single focal length. We find that it offers reasonable approximation of our shallow lens structure, and as shown later the calculated results agree well with the experiments within errors. For a thin spherical lens with diameter D and thickness h, the radius of curvature R is given by

$$R = D^2/8h + h/2. \tag{1}$$

The lens volume [see Fig. 3(d)] is

$$V_0 = \pi R^3(\cos^3\theta - 3\cos\theta + 2)/3, \tag{2}$$

and the curved-surface area of the lens A [see Fig. 3(c)] is

$$A = 2\pi R^2(1-\cos\theta), \quad \text{where } \theta = \sin^{-1}(D/2R). \tag{3}$$

Therefore, the focal length f in terms of A and D can be derived as

$$f = \frac{R}{n-1} = \frac{A}{2\pi(n-1)\sqrt{\frac{A}{\pi} - \frac{D^2}{4}}}, \tag{4}$$

where n is the refractive index of the lens material, here, the PDMS bilayer. Under stretching with an applied strain ε, the lens diameter changes from D to $D(1+\varepsilon)$, and the focal length f of a stretched lens becomes

$$f = \frac{A}{2\pi(n-1)\sqrt{\frac{A}{\pi} - \frac{D^2(1+\varepsilon)^2}{4}}}. \tag{5}$$

The curved-surface area of the concave lens can be written in terms of the base area as $\pi D^2(1+\varepsilon_0)^2/4$, where the value of ε_0 is obtained from initial lens profile by comparison of the base area and the curved-surface area [Fig. 3(c)]. When the lens is stretched in both planar directions simultaneously, both the base area and the curved surface area increase. When ε approaches to the prestrain ε_P, the lens becomes completely flat, that is, the base area and the curved surface area should become equal. Although there is a hard thin coating of oxide (<50 nm) on PDMS in the buckled structure, we believe that the oxide deforms together with the underlying PDMS film when stretched. In the lens structure reported here, the fact that a very thin lens (h=1.53 μm and D =45.9 μm) was formed after releasing a prestrain of 20% suggests that the area of the oxide layer should not remain fixed during the stretching/release. Thus, the curved surface area A increases until it becomes equal to the base area at

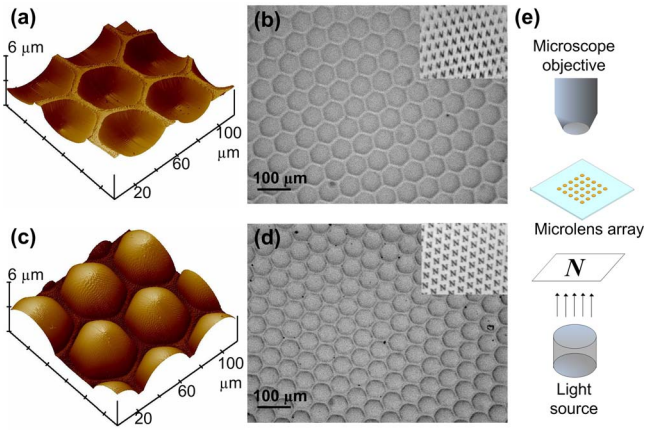

FIG. 2. (Color online) AFM images of (a) concave and (c) convex microlens array. Optical images of (b) concave and (d) convex microlens arrays, corresponding to those from (a) and (c). Insets: the optical images of letter "N" imaged through the respective microlens arrays. (e) Optical setup for measuring the microlens focal length.

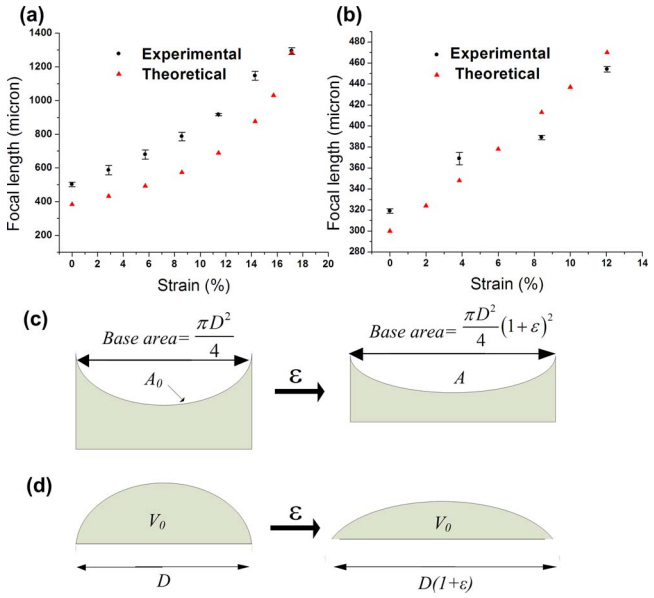

FIG. 3. (Color online) Focal length variation and corresponding stretching mechanism of the concave [(a), (c)] and convex [(b), (d)] microlens arrays, respectively.

prestrain. This condition is satisfied when the curved surface area A is approximated by

$$A = \frac{\pi D^2}{4}\left(1 + \frac{\varepsilon_P - \varepsilon_0}{\varepsilon_P}\varepsilon + \varepsilon_0\right)^2. \quad (6)$$

From Eqs. (5) and (6), we can calculate the focal length of concave microlens as a function of the applied strain ε.

In the case of stretching the convex microlens, the lens diameter D increases and lens height h decreases to maintain constant lens volume V_0 [Fig. 3(d)]. Therefore, the convex lens can never become completely flat, and the focal length f as a function of strain ε is given by the solution of the following equation:

$$f^3 - \left[\frac{\pi D^4(1+\varepsilon)^4}{64(n-1)V_0}\right]f^2 - \left[\frac{\pi D^6(1+\varepsilon)^6}{768(n-1)^3V_0} + \frac{3V_0}{4\pi(n-1)^3}\right] = 0. \quad (7)$$

As seen in Fig. 3(a), the focal length of concave microlens array increases rapidly when the strain ε approaches to the prestrain ε_P (20%): 83% increase of focal length experimentally at $\varepsilon=12\%$ and 158% increase at $\varepsilon=17\%$. In the case of convex microlens array, only 42% increase of focal length is observed at $\varepsilon=12\%$ [Fig. 3(b)].

The significant difference in the tunability of the concave and the convex microlens array may be explained by the fundamental difference in the origin of lens formation. The curved structure of the concave microlenses is formed under the buckling force when the prestrain ε_P is released after formation of oxide layer. Thus, by design, the concave microlens should be completely flattened, i.e., the lens volume V decreases to zero when the applied strain becomes equal to the presstrain, ε_P. This constraint of $V=0$ at $\varepsilon=\varepsilon_P$ in the concave lens provides large tunability of the focal length by applying mechanical strain. In contrast, the curved structure of the convex microlens is replicated from the concave microlens and there is no buckling involved in lens formation. When a convex microlens is stretched, since PDMS is an elastomer (Poisson's ratio $\nu\approx0.5$), the lens volume V_0 remains constant such that the lens can never become completely flat. This constraint results in considerably smaller focal length tunability.

To estimate the focal length, we assumed the lenses were spherical with either completely flat lens at prestrain (concave lens) or constant lens volume (convex lens) constraints. In comparison of the experimental and calculated focal length versus applied strain, we observed similar trend but systematic difference in the concave microlenses [Fig. 3(a)], whereas those agree reasonably well in the convex microlenses [Fig. 3(b)]. It suggests that our approximation is sound. The systematic difference between the experimental and theoretical data in concave lenses may be partially attributed to the difference in refractive indices in the bilayer structure, which is not taken into account in calculation due to the uncertainty in thickness of the oxide layer. In addition, Eq. (6) for curved surface area as a function of strain may not be accurate enough to approximate the actual change in lens surface area with increase of strain.

In conclusion, using mechanical strain induced buckling on patterned PDMS bilayers and replica molding, we fabricated concave and convex microlens arrays, respectively. We demonstrated strain responsive, real-time focal length tunability of both types of microlens array. Due to the difference in the mechanism of lens formation, the concave and convex microlens array showed fundamentally different strain response behaviors. Larger range of focal length tunability was obtained from concave lens array than that from convex lens array. We believe that the fabrication of single-component, strain-responsive microlens arrays and study of their tunability would offer important insights to design tunable optical microdevices for many optics, MEMS, and sensing applications.

This work is supported by the National Science Foundation (No. BES-0438004) and ACS PRF G (Grant No. 43336-G7). S.Y. would also thank the 3M Nontenured Faculty Grant.

[1] J. Kim, S. Nayak, and L. A. Lyon, J. Am. Chem. Soc. **127**, 9588 (2005).
[2] S. Yang, C. K. Ullal, E. L. Thomas, G. Chen, and J. Aizenberg, Appl. Phys. Lett. **86**, 201121 (2005).
[3] L. A. Dong, A. K. Agarwal, D. J. Beebe, and H. R. Jiang, Adv. Mater. (Weinheim, Ger.) **19**, 401 (2007).
[4] S. Yang, T. N. Krupenkin, P. Mach, and E. A. Chandross, Adv. Mater. (Weinheim, Ger.) **15**, 940 (2003).
[5] N. Chronis, G. L. Liu, K. H. Jeong, and L. P. Lee, Opt. Express **11**, 2370 (2003).
[6] H. W. Ren, Y. H. Fan, and S. T. Wu, Opt. Lett. **29**, 1608 (2004).
[7] K. S. Hong, J. Wang, A. Sharonov, D. Chandra, J. Aizenberg, and S. Yang, J. Micromech. Microeng. **16**, 1660 (2006).
[8] P. Lin and S. Yang, Appl. Phys. Lett. **90**, 241903 (2007).
[9] N. Bowden, W. T. S. Huck, K. E. Paul, and G. M. Whitesides, Appl. Phys. Lett. **75**, 2557 (1999).
[10] E. P. Chan and A. J. Crosby, Adv. Mater. (Weinheim, Ger.) **18**, 3238 (2006).